Available online at www.sciencedirect.com

ScienceDirect

Procedia Structural Integrity 2 (2016) 2936–2943

Structural Integrity Procedia

www.elsevier.com/locate/procedia

21st European Conference on Fracture, ECF21, 20-24 June 2016, Catania, Italy

Prediction of ductile fracture in anisotropic steels for pipeline applications

T. Coppola[a]*, F. Iob[a], L. Cortese[b], F. Campanelli[c]

[a]*Centro Sviluppo Materiali S.p.A. (CSM), via di Castel Romano 100, 00128 Rome, Italy*
[b]*Faculty of Science and Technology, Free University of Bozen, piazza Università, 5, 39100 Bolzano, Italy*
[c]*D'Appolonia S.p.A., via Cesare Pavese, 305, 00144 Rome, Italy*

Abstract

Large diameter steel pipelines for gas transportation may experience extreme overloads due to external actions such as soil sliding, faults movements, third part interactions. In these scenarios the material undergoes severe plastic strains which locally may reach the fracture limits. Due to the manufacturing process, the steels used in such applications have an anisotropic behavior both for plasticity and fracture. In this paper two steel grades have been characterized in view of anisotropic plastic fracture. Fracture tests have been planned to characterize the fracture behavior under different stress states and in different directions to define the anisotropic sensitivity. Finite element modelling, incorporating an anisotropic plasticity formulation, has been used to calculate the local fracture parameters in the specimens and to define the complete ductile fracture locus. An uncoupled damage evolution law has been finally used to evaluate the fracture limits on real pipelines failed in full scale laboratory tests. The strain to fracture prediction has been verified by local strain measurements on the fractured pipes. The model robustness has been also verified on global parameter predictions, such us the burst pressure.

Peer-review under responsibility of the Scientific Committee of ECF21.

Keywords: ductile fracture; anisotropic plasticity; onshore pipelines

* Corresponding author. Tel.: +39-06-5055362; fax: +39-06-5055452.
E-mail address: t.coppola@c-s-m.it

Copyright © 2016 The Authors. Published by Elsevier B.V. This is an open access article under the CC BY-NC-ND license (http://creativecommons.org/licenses/by-nc-nd/4.0/).
Peer review under responsibility of the Scientific Committee of ECF21.
10.1016/j.prostr.2016.06.367

1. Introduction

Offshore and onshore pipelines may experience extreme loading conditions during their installation and operation, both of monotonic and cyclic nature. Loading actions such as pipeline lateral displacements, tensioning, or external damage by third part interaction combined with internal or external pressure, may trigger undesirable local or global deformation modes, like section collapse, bulging, wrinkling and denting. Such extreme events require a robust modelling approach to analyse scenarios not covered by current codes.

Large diameter steel gas pipelines up to 56" are produced by thermo-mechanical controlled hot rolling and accelerated cooling (TMCP process) of plates with thickness which may range, according to the product, from 15 to 30 mm. The plates manufacturing rolling process develops anisotropy in the final product and also develops an amount of work hardening which is not fully recovered during cooling, with a retained anisotropic structure and elongated grains in the rolling direction. The plate final mechanical properties are so anisotropic as well. Further cold working is applied during the so called UOE shaping (Vathi, 2011) where the material undergoes to cold straining in specific directions, such as bending in the U and O shaping or circumferential expansion in the final calibration step.

Nomenclature

a_i anisotropic coefficients
f triaxiality function for damage
g deviatoric function for plasticity
h generalized Hill48 yield function
n hardening coefficient
p hydrostatic pressure
q von Mises stress
r Lankford coefficient
$G(X)$ deviatoric function for damage
H_i yield stress ratios
J_2 second invariant of deviatoric stress tensor
J_3 third invariant of deviatoric stress tensor
S yield function
T triaxiality parameter
X deviatoric parameter
ε_p equivalent plastic strain
ε_{ij} strain tensor
σ_{ij} stress tensor
θ Lode angle
β material plasticity parameter
γ material plasticity parameter
β_D material damage parameter
γ_D material damage parameter

The final mechanical properties of UOE pipes are known to be strongly different along the material principal axis, which in this case are also coincident with the pipe's ones. Two aspects have to be considered in the material behavior. The first deals with plasticity, which has been demonstrated to be anisotropic both for yielding and hardening, additionally including the Lode angle dependence. This aspect has been widely described in the paper of Iob et al. (2015) where a modified Hill48 plasticity criterion has been presented. The second aspect regards the

fracture behavior in anisotropic materials, which can be not only dependent from the stress state (triaxiality and Lode angle) but also from the material orientation.

In this paper, experiments are carried out on pipeline steels API X80 (48”x19 mm Pipe) and X70 (56”x22 mm Pipe) grades in the as received state. Tensile tests are carried out on round and notched bars specimens extracted from the pipes along various directions (referred to the pipe axis) to study the anisotropy of the material. Torsion tests have been also tested in different directions both for plasticity and fracture characterization. Tensile tests in plane strain state on plates with notch have finally performed for special stress state characterization. The new material constitutive equation described in Iob et al. (2015), incorporating plastic anisotropy and Lode angle dependency, together the fracture locus modelling according to Coppola (2009) are used to define the fracture resistance in the two anisotropic steels. The model capability on ductile fracture evaluation has been proved on the prediction of the burst pressure on full scale internal pressure failure tests performed on API X70 and X80 pipeline steels.

1. Anisotropic plasticity material model and fracture locus model

When the material has an orthogonal symmetry along the three principal anisotropic axes *x, y, z*, Hill (1948) proposed a generalization of the von Mises yield criterion named Hill48 (eq.1):

$$F\left(\sigma_y-\sigma_z\right)^2+G(\sigma_z-\sigma_x)^2+\mathrm{H}\left(\sigma_x-\sigma_y\right)^2+2L\tau_{yz}^2+2M\tau_{zx}^2+2N\tau_{xy}^2=1 \tag{1}$$

where the six constants F, G, H, L, M, N can be expressed in terms of the yield point stresses in uniaxial tension, σ_{0x}, σ_{0y}, σ_{0z}, and the yield point stresses in shear τ_{0xy}, τ_{0yz}, τ_{0zx}.

Under the plane stress hypothesis, usually applied for sheet characterization, the six Hill coefficients are reduced to four and can be obtained by tensile tests carried out on specimens extracted on the loading plane aligned on three direction: $\theta=0°$, $\theta=45°$ and $\theta=90°$. No experimental tests in thickness direction *z* are needed and yield in this direction is calculated from experimental information in the *xy* plane directions.

The limit of this simplified formulation is that the hypothesis of plane stress condition could be not realistic in the cases of not negligible plate thickness, leading to some errors in the calculation of the through thickness yield of the material and in the identification of the shear coefficient of Hill48 formulation. Another limit is that the coefficients used in the Hill48 criterion are constant and so it isn’t possible to characterize the different strain hardening that the anisotropic material exhibit in the different directions. Finally, the Hill48 criterion doesn’t take into account any Lode angle effect, otherwise expressed by the J_3 dependence.

To overcome the above limitations, the Hill48 function has been extended (Iob, 2015) by considering the complete description of yielding and hardening in the six directions, including the Lode angle effect for the shear stress states according to the formulation of Bigoni and Piccolroaz (2004) with the generalization of Coppola et al. (2013). The yield function according to the new criterion, named M-Hill48, is expressed by:

$$S=\frac{h(\varepsilon_p)}{g(\theta,\varepsilon_p)} \tag{2}$$

$$h(\epsilon_p)=\frac{1}{\sqrt{2}}\sqrt{a_1(\epsilon_p)\left(\sigma_y-\sigma_z\right)^2+a_2(\epsilon_p)(\sigma_z-\sigma_x)^2+a_3(\epsilon_p)\left(\sigma_x-\sigma_y\right)^2+3a_4(\epsilon_p)\tau_{zx}^2+3a_5(\epsilon_p)\tau_{yz}^2+3a_6(\epsilon_p)\tau_{xy}^2} \tag{3}$$

The function *h* is the complete Hill48 criterion with variable coefficients a_i that can be calculated by the ratio of the tensile and shear yields measured in the three orthogonal directions of the material. Due to the difficulties to perform pure shear stress tests up to strain to failure, by introducing the Mohr relations we can obtain the shear stresses from three tensile tests carried out in the 45° orientations between the anisotropic principal axis. So, the complete 3D formulation of the yield criterion needs six independent experimental tensile tests carried out in the

three principal anisotropic directions and in the three 45° directions between each axis pair. The function $g(\theta)$ is defined as:

$$g(\theta)=\left[\cos\left(\beta\frac{\pi}{6}-\frac{1}{3}\arccos\left(\gamma\cos(3\theta)\right)\right)\right]^{-1} \tag{4}$$

with $\cos(3\theta)=\frac{27}{2}\frac{J_3}{q^3}$ and $\theta\in\left[0;\frac{\pi}{3}\right]$. The angle θ assumes extreme values for specific stress states. $\theta=0$ is obtained for tensile stress states, $\theta=\pi/3$ for compressive ones and $\theta=\pi/6$ for pure shear and plane strain states. Intermediate values correspond to mixed stress states. Through the function $g(\theta)$ it is possible to model the shape of the yield surface deviatoric section. The extension to the case with variable parameters β and γ has also been applied, both depending by the current plastic strain ε_p (see Coppola et al., 2013; Cortese et al. 2016). Being the function *h* convex, as the function *g* doesn't introduce inflections if $\beta\in[0;2]$ and $\gamma\in[0;1)$ the same occurs for the new function *h/g*, so the convexity for *S* is also verified. Derivatives are also continuous within the same ranges, as demonstrated by Bigoni (2004).

The anisotropic plasticity model is complemented with a standard uncoupled ductile damage model (Coppola et al., 2009), which takes into account for both stress triaxiality *T* and Lode angle sensitivity. The main keystones in the damage framework proposed are: i) plasticity and damage are uncoupled; ii) the matrix is always hardening; iii) damage evolution is stress state dependent through triaxiality and deviatoric parameters. The damage model is described by:

$$D=\int_0^{\varepsilon_f}\frac{f(T)}{G(X)^{1/n}}d\varepsilon_p \tag{5}$$

$$f(T)=C_1e^{C_2T} \tag{6}$$

$$G(X)=\frac{\alpha}{\cos\left[\beta_D\frac{\pi}{6}-\frac{1}{3}\cos^{-1}\left(\gamma_D X\right)\right]} \tag{7}$$

Damage accumulates according to the eq. (5) in which triaxiality $T=p/q$ and deviatoric X functions are defined in eq. (6) and (7). To note that the deviatoric parameter is $X=\cos(3\theta)$ as defined before. The damage model proposed is a generalization of the Bao one (2004). To note that the deviatoric function *G* in eq. (7) is similar to the function *g* used in eq. (4) but is only referred to the fracture locus description. Also the material parameters β_D and γ_D have a similar meaning to β and γ used in eq. (4) but are only referred to the fracture locus. The fracture locus is defined by a bound with a plastic strain value at failure depending by a specific (*T, X*) pair.

In case of monotonic and proportional loading the values *T* and *X* are constant along the straining path. In non-proportional loading *T* and *X* are variable, but eq. (5) may be still used for a specific straining path by using actual variable values. The fracture point is characterized by a (*T, X*) pair where their values is the effective one, as indicated by Bao (2004), Coppola (2009) and Cortese (2014).

2. Materials, mechanical testing and experimental procedures

Two steel grades obtained from large diameter pipelines for gas transportation are considered, the first one is an API X70 grade, 56" outer diameter and 22.3 mm wall thickness, the second one is an API X80 grade, 48" outer diameter and 19.8 mm wall thickness. The material anisotropy was characterized by tensile tests carried out in the base material of the pipe with tensile specimens extracted in six different orientation (Iob et al. 2015). Three standard tensile test, with geometry according to UNI EN ISO 6892-1:2009 are carried out on round bar smooth specimen having 9 mm gauge section diameter, extracted in the longitudinal (L), transversal (T) and 45° degrees between L-T directions (45°LT) of the pipe. Three tensile tests are carried out on round specimen having 2.5 mm gauge section diameter extracted in the through thickness direction of the pipe (N), and oriented at 45° degrees from longitudinal and trough thickness direction (45°LN) and at 45° degrees from transversal and trough thickness

direction (45°TN). Load and gauge section elongation have been measured and registered by load cell and extensometer up to the specimen fracture. Three tests for each direction have been performed to verify the repeatability. Load-displacement curves in the six directions have been next elaborated to obtain the true stress-strain curves up to necking. To analyze the material behavior under shear loading, torsion tests have been carried out on round specimens extracted in longitudinal (L) and circumferential (T) directions of the pipes. The torsion specimens have a 8 mm diameter and 20 mm length test section.

Round notch bar specimens have been cut in the L and T direction from both pipes. Two geometries have been studied, RNB3 having a minimum section of 9 mm and a notch radius of 3 mm, and RNB15 having a minimum section of 7.5 mm and a notch radius of 15 mm.

Finally flat notched specimens (PSN), with transvers section of 60x15 mm and a half circle notch with 1 mm radius at the extrados, have been cut from the longitudinal direction for tensile testing up to fracture.

Smooth tensile (RB), notched tensile (RNB) and flat tensile notched (PSN) tests have been performed up to fracture by registering the load and clip gauge displacement for subsequent elaboration.

3. Model parameters identification

Plasticity model parameters for the two steel grades under investigation have been extensively described in Iob et al. (2015), so won't be presented here again.

The identification of the damage model parameters for materials X70 and X80 has been performed by using results from tensile tests (RB and RBN), torsion tests and flat tensile tests with notch (PSN). Each test has been reproduced by FE (*MSC.Marc* code), calculating the two stress parameters T and X along the strain path and using the plasticity model described in previous section. As first hypothesis, an isotropic damage accumulation law has been postulated. To perform calculations, a CSM proprietary routine has been used. Next the equivalent plastic strain and the parameters T and X have been extracted and plotted for the critical points in each specimen type up to the fracture point detected by the experimental tests (typically shown by the load drop in the load-displacement diagram). The local displacement at fracture has been used as final point in the simulation to evaluate the plastic strain and for computing the effective values T and X in the strain path. The values for plastic strain, T and X obtained for the two steel grades are listed in Table 1.

Some scatter in the fracture strain is observed in torsion tests and in round bar tests (RB), indicating some dependency from the direction (see Fig. 1), while this is not observed in the notched specimens (RNB15 and RNB3). So the fracture model has been fitted with the standard eq. (5) for the isotropic case. Damage model parameters for eq. 6 and 7 fitted on experiments in Table 1 are reported in Table 2.

Table 1. Fracture locus points for X70 and X80 grades.

	X70			*X80*		
Test	ε_f	T_m	X	ε_f	T_m	X
RB-L	1.22	0.51	1	1.32	0.52	1
RB-T	1.12	0.49	1	1.21	0.51	1
RB-45	1.50	0.46	1	1.60	0.62	1
RB-R	1.48	0.58	1	1.47	0.69	1
RNB15-L	0.87	0.69	1	1.04	0.74	1
RNB15-T	0.84	0.66	1	1.04	0.72	1
RNB3-L	0.48	1.09	1	0.52	1.16	1
RNB3-T	0.60	1.02	1	0.52	1.07	1
Torsion L	1.71	0	0	1.60	0	0
Torsion T	1.38	0	0	1.72	0	0
PSN-L	0.64	0.62	0.31	0.48	0.65	0.35

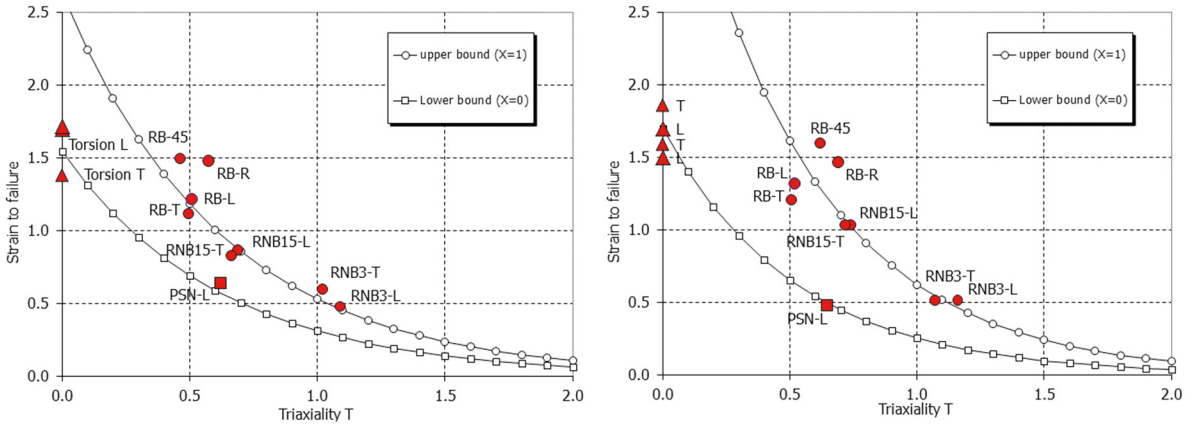

(a) (b)

Fig. 1. (a) fracture locus for X70; (b) fracture locus for X80.

Table 2- Damage model parameters for X70 and X80.

Damage model parameter	*X70*	*X80*
C_1	0.38	0.24
C_2	1.60	1.90
n	0.27	0.16
α	0.866	0.866
β_D	1	1
γ_D	1	1

4. Model validation

Two full scale tests under monotonic loading aiming to reproduce extreme loading scenarios on pipelines have been performed to validate the approach. In the first case a 48” diameter pipeline with 19.8 mm thickness in X80 steel grade is considered. The loading mode is bending followed by increasing internal pressure up to burst. The scenario aims to reproduce the condition of a pressurized pipeline subject to lateral displacement during a soil sliding with subsequent damage induced by local buckling, followed by an over pressure. So the loading mode reproduced in full scale testing is four point bending followed by increasing pressure up to burst. The total pipe length used is 12 m, the loading jacks span is 8.2 m, the fixed points span is 28.8 m, including dummy prolongations. The pipe was initially pressurized at 108 bars, next loaded in bending up to instability. The bent pipe has been cut and machined at the ends for the end cap welding, next pressurized up to burst with water. Both bending test and burst test have been performed at the CSM full scale test facilities.

The second case is a 56” diameter pipeline with 22.3 mm thickness in X70 grade. The loading mode is increasing pressure up to burst on artificially reduced thickness simulating diffused corrosion. The scenario aims to reproduce the condition of a locally corroded pipeline after long term service subject to an over pressure. The pipe was prepared by end cap welding for pressure application. To simulate diffuse corrosion, a 7 mm thickness reduction (metal loss) has been machined at the mid-section, 45° circumferential position with respect to the longitudinal welding on a 700x50mm wide area. The thickness reduction and material removal dimensions have been selected by using indications from DNV-RP-F101.

Both full scale tests have been modelled by using the FE code *MSC.Marc*. Three dimensional schematization with 8 node brick linear elements (full integration) has been used. Cavity elements have been used to calculate the

water filling volume. The material behavior is anisotropic with plastic damage accumulation according to model described in section 2.

In the first case the model is formed by two load steps. In the first step the pipe is bent (four point bending) with internal pressure (p=108 bar) to form the wrinkle in the intrados, in the second step the pipe is pressurized up to burst. The maximum pressure at instability from simulation is 241 bar, to be compared with that reached during the test of 240.5 bar. The plastic strain at failure was measured by the thickness reduction on the necked section. The failure point has been located on the fracture locus reconstructing the stress history by FEM and determining the mean T and X values. The result is shown in Figure 2. It can be seen in Fig. 2 (a) that the measured failure point is placed on the FEM predicted limit curve (X=0.55, T=0.42). To note that the pipe failure is not located in the point where the plastic strain is higher (the wrinkle) but at the bulging point near the extrados, as shown in Fig. 2 (b).

In the second case a single pressurizing step up to burst is modelled. The experimental plastic strain to failure has been determined by the deformation of an electro-chemically etched square grid placed on the reduced thickness zone before the testing, as shown in Fig. 3 (a). The maximum strain calculated by the model in Fig. 3 (b) is very close to than measured in Fig. 3 (a). It can be seen in Fig. 4 (a) that the measured failure point is placed on the FEM predicted limit curve (X=0.1, T=0.6), corresponding to a near plane strain condition, as also verified in Fig. 3 (a). The maximum pressure at instability from simulation is 156.8 bar, to be compared with the experimental burst pressure of 156.3 bar, as shown in Fig. 4 (b).

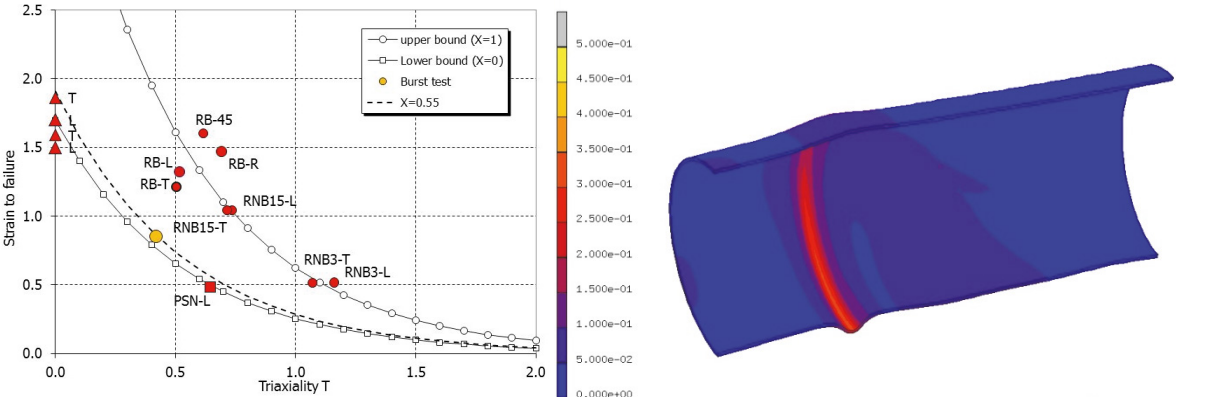

(a) (b)

Fig. 2. (a) fracture locus for X80 grade with experimental test failure point; (b) plastic strain distribution in full scale test simulation

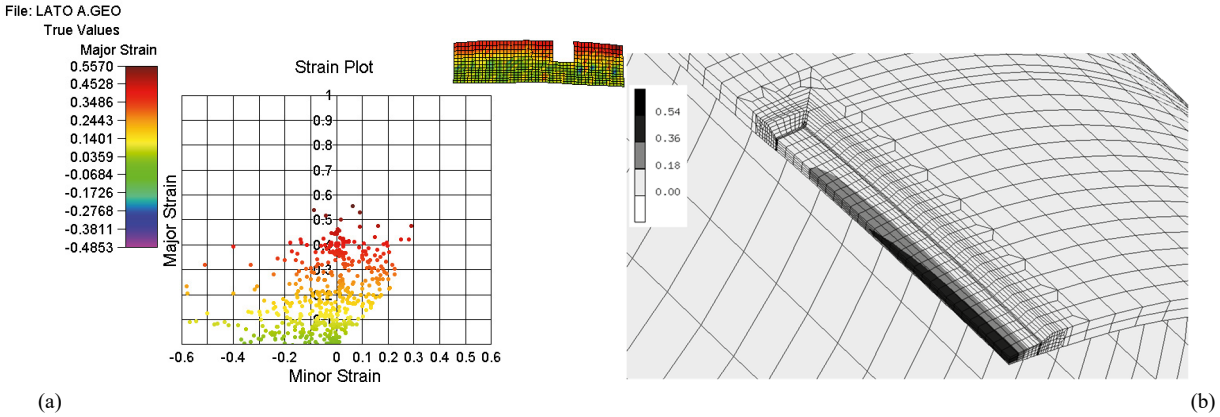

(a) (b)

Fig. 3. (a) strain map measured on fracture region of X70 full scale test; (b) plastic strain distribution calculated by FEM.

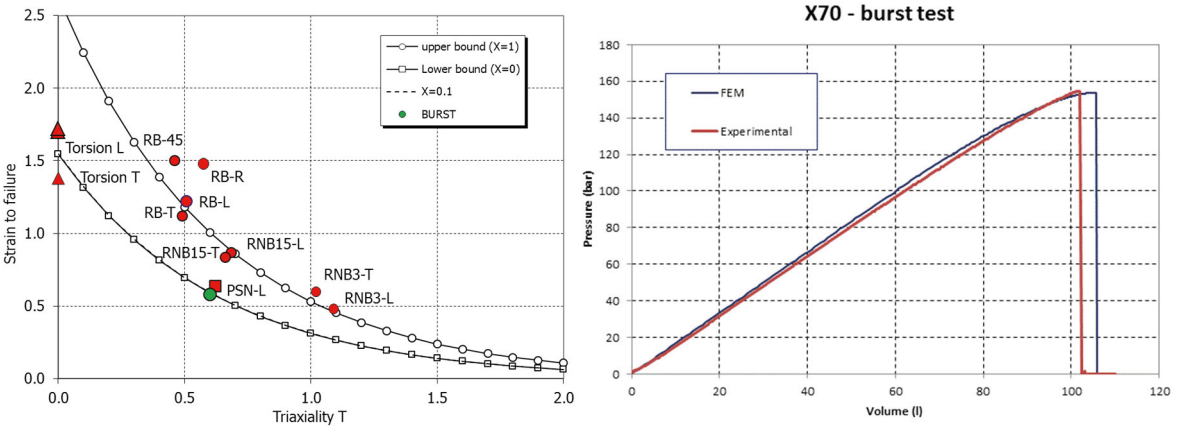

(a) (b)

Fig. 4. (a) fracture locus for X70 grade with experimental test failure point ; (b) volume fill *vs* pressure comparison in full scale burst test between experimental and numerical prediction by FEM.

5. Conclusions

A recently developed anisotropic plasticity model, extending to the complete three-dimensional case the standard Hill48 formulation and including non-uniform hardening and Lode angle dependence, has been used together a conventional isotropic plastic damage model in the study of pipelines failure under extreme loading conditions. The model predictions have been validated against local parameters, such as plastic strain at the failure point, and on global parameter predictions, such us the burst pressure. The isotropic damage model coupled with the anisotropic plasticity model has been proved to be precise enough for the fracture prediction in real scenarios.

Acknowledgements

Part of the experimental and numerical activities were carried out with a financial grant of the Research Programme of the Research Fund for Coal and Steel, Contract N. RFSR-CT-2011-00029, project acronym *ULCF*.

References

Bao, Y., Wierzbicki, T., 2004. On Fracture Locus in the equivalent Strain and Stress Triaxiality Space, Int. Journal of Mech. Sciences 46, 81-98.

Bigoni, D, Piccolroaz, A., 2004. Yield Criteria for Quasi Brittle and Frictional Materials. International Journal of Solids and Structures 41, 2855-2878.

Coppola, T., Cortese, L., Folgarait, P., 2009. The Effect of Stress Invariants on Ductile Fracture Limit in Steels, Engineering Fracture Mechanics 76, 1288-1302.

Coppola, T., Cortese, L., Campanelli, F., 2013. Implementation of a lode angle sensitive yield criterion for numerical modelling of ductile materials in the large strain range. Computational Plasticity XII: Fundamentals and Applications - Proceedings of the 12th International Conference on Computational Plasticity - Fundamentals and Applications, COMPLAS 2013, 1097-1108.

Cortese, L., Coppola, T., Campanelli, F., Campana, F., Sasso, M., 2014. Prediction of ductile failure in materials for onshore and offshore pipeline applications. International Journal of Damage Mechanics 23(1) 104-123.

Cortese, L., Coppola, T., Campanelli, F., Broggiato, G.B., 2016. A J2-J3 approach in plastic and damage description of ductile materials. International Journal of Damage Mechanics 25(2), 228-250.

Hill, R., 1948. Theory of yielding and plastic flow of anisotropic metals. P R Soc. A 193, 281-297.

Iob, F., Campanelli, F., Coppola, T., 2015. Modelling of anisotropic hardening behavior for the fracture prediction in high strength steel line pipes, Engineering Fracture Mechanics 148, 363-382.

Vathi, M., Karamanos, S.A., 2011. Finite Element modelling of UOE pipe manufacturing process, Proceedings of the 7th National Conference on Metal Structures, Volos, Greece.